F. J. Asensio, J. I. S. Martín, I. Zamora, O. Oñederra, G. Saldaña and P. Eguia, "*A system approach to harnessing wind energy in a railway infrastructure,*" **IECON 2018 - 44th Annual Conference of the IEEE Industrial Electronics Society, Washington, DC, USA, 2018**, pp. 1646-165. https://doi.org/10.1109/IECON.2018.8591777

A system approach to harnessing wind energy in a railway infrastructure

F.J. Asensio[1], J.I. San Martín[1], I. Zamora[2], O. Oñederra[2], G. Saldaña[1], P. Eguia[2]
Department of Electrical Engineering – University of The Basque Country (UPV/EHU)

[1]Engineering Schoool of Gipuzkoa
Avda. Otaola, 29, 20600 Eibar (Spain)
franciscojavier.asensio@ehu.eus

[2]Engineering School of Bilbao
Alda. Urquijo s/n, 48013 Bilbao (Spain)
inmaculada.zamora@ehu.eus

***Abstract*—This paper focuses on a system approach aimed at harnessing the wind potential in a railway infrastructure. The key aspect of the proposed system lies in using the mass of air displaced during the movement of a train along a railway track to produce electrical energy. Through the use of techniques based on Geographic Information Systems (GIS) and Finite Element Method (FEM) simulations, the optimal location of the mini Vertical Axis Wind Turbines (VAWT) has been chosen, taking into account the speed of the train, the railway sections without obstacles and the speed and direction of the wind. The proposed conversion system to integrate the system consists of a low voltage AC/DC stage and a DC/DC stabilization stage per wind generator, and an isolation stage based on a Solid State Transformer (SST), which connects all the generators and allows to inject the energy generated to the medium voltage DC catenary.**

Keywords—wind energy harnessing, RES integration, solid state transformer, MVDC link.

I. INTRODUCTION

Actually, due to the existing energy problem, a change of attitude is taking place regarding the care of the environment, thanks to which renewable energies have begun to gain presence both at a private and public level, appearing in industry sector as well as in public institutions and infrastructures.

In this context, there is a growing interest in improving the energy efficiency of transport systems. The rail system is among one of the most suitable transportation systems because it is an ecological means of transport that, through the use of renewable energy, allows the reduction of polluting emissions into the atmosphere [1]. In addition, the introduction of new technological developments can help reduce energy consumption and increase the energy efficiency of this means of transport.

Over the last few years, one of the improvements in the energy efficiency of railway systems has come through the application of regenerative braking of electric traction vehicles, so that the kinetic energy of the braking of such vehicles can be converted into usable electrical energy [2]-[4].

Other research works and developed projects have studied the flow of air displaced by a train and suggest the use of available wind energy due to the displacement of air mass produced when the train circulates inside a tunnel [5]-[6]. However, despite the fact that the effect of speed is magnified inside a tunnel, when there is no train in motion, the wind turbines do not produce energy, thus reducing its utilization factor and thus increasing the payback of the system.

The location of the system of generation in sections of track in which the train circulates on the outside allows to maximize the utilization factor of the system, since the wind generators are able to generate even when there is no train circulation. However, the integration of renewable energies into MVDC systems requires the study of connection topologies that allow these systems to operate properly without impairing the correct functioning of the whole system [7].

Considering all of the above-mentioned facts, this paper proposes a system approach to harnessing wind energy in a railway of the subway of Bilbao (Spain). In this sense, a study on the available wind resource and the potential of the air mass displaced by the train has been done, the optimal location for a generation system based on Vertical Axis Wind Turbines (VAWTs) has been chosen, and a power conversion system to integrate the VAWTs into the MVDC catenary has been proposed.

II. OPTIMAL LOCATION AND WIND RESOURCE

To set the optimal location of the VAWTs, a GIS (Geographic Information System) technique has been used. In this sense, maps of wind speed, subway tracks, satellite view and orography of the location have been superimposed. For the case of the map

of wind speed, the global wind atlas of 1 km resolution provided by International Renewable Energy Agency (IRENA) has been used [8].

A. *Optimal location*

Fig. 1 shows the overlapping of the maps of the wind resource at 50 meters high and the underground and aboveground tracks.

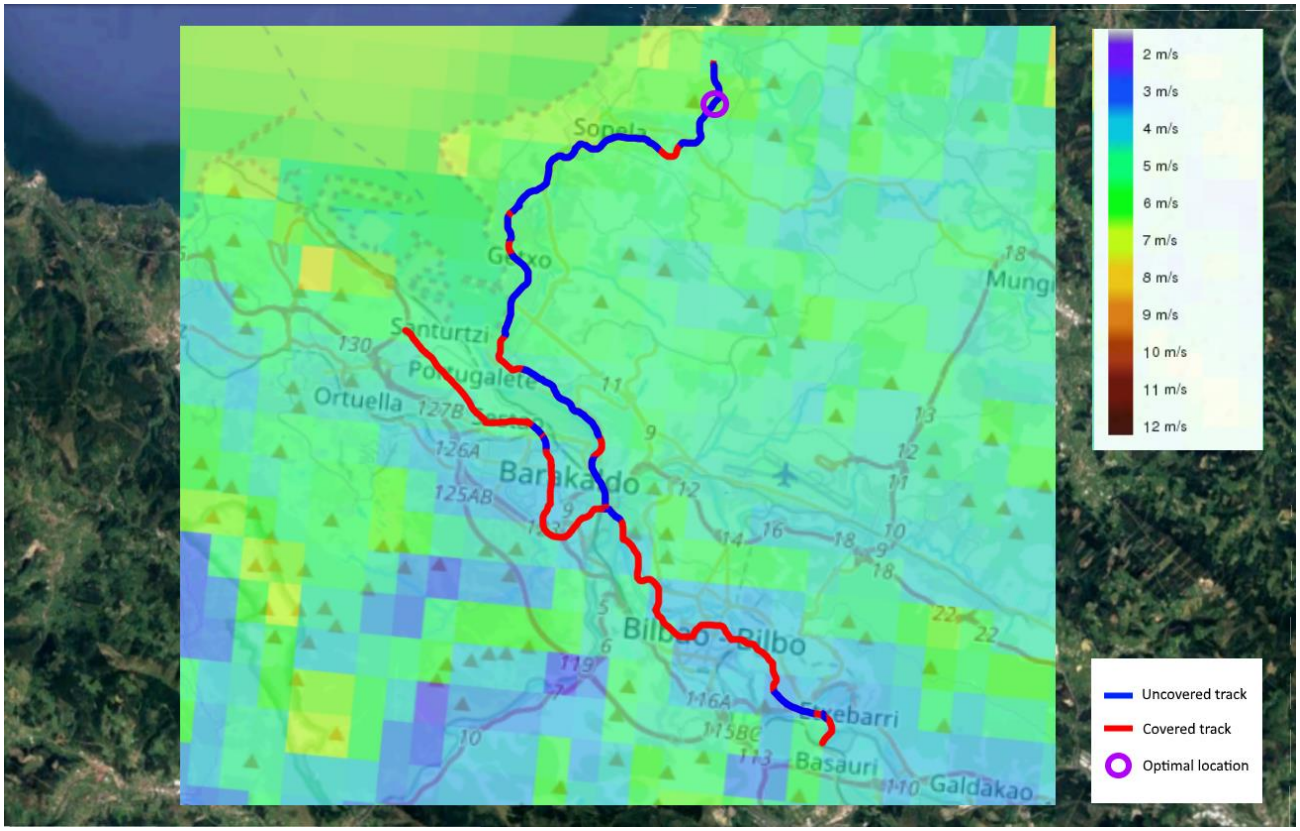

Fig. 1. Overlay of maps of wind speed and underground and aboveground tracks.

Below are described the factors that have been considered to select the optimum location.

1) *Aboveground tracks.* The aboveground tracks are taken into account to produce energy when the train does not pass.
2) *Train speed*. The greater the speed of the train, the greater the speed reached by the displaced air mass.
3) *Number of train tracks.* With a single train track, it is possible to take better advantage of the air mass displaced by the train when it circulates in both directions (it can be installed VAWTs on both sides of the track).
4) *Proximity to power substations*. The proximity of a power substation capable of evacuating the power generated by the VAWTs when the subway is not operating to minimize power losses.
5) *Available space.* Land space available for optimal installation of each VAWT.
6) *Wind resource*. The higher the wind speed, the greater the total electric power produced.
7) *Wind direction.* The prevailing wind direction determines the amount of space needed, since the turbines will be distributed perpendicular to that direction.
8) *Obstacles.* The minimum number of obstacles that can stop the wind that reaches the turbines or may divert its path by creating turbulences, such as trees, hills or buildings.

Considering all the factors mentioned above, the geographical location indicated in Fig. 1 has been chosen (latitude: 43º23’22.3’’ N, longitude: 2º56’43.24’’ O).

The area chosen is an unobstructed location, it comprises a section of a single straight and uncovered train track of 255 m in length, in which the train reaches its maximum velocity of 80 km/h. In regard to the proximity to a power substation, it is 3 km away from the nearest substation through which energy could be evacuated to the power grid when the train does not operate. Moreover, the wind conditions in the area chosen are suitable, being the predominant direction ONO. In this sense, the VAWTs will be located along the train track with 70° difference with respect to the predominant wind direction.

Given that the minimum distance to maintain between each turbine is three diameters on the sides and five diameters between turbines arranged in parallel to the prevailing wind direction, it is concluded that necessary space conditions are met to install 10 VAWTs, half on each side of the railway. Fig. 2 shows a representative scheme of the VAWT connection with the power conversion unit and the catenary of the train.

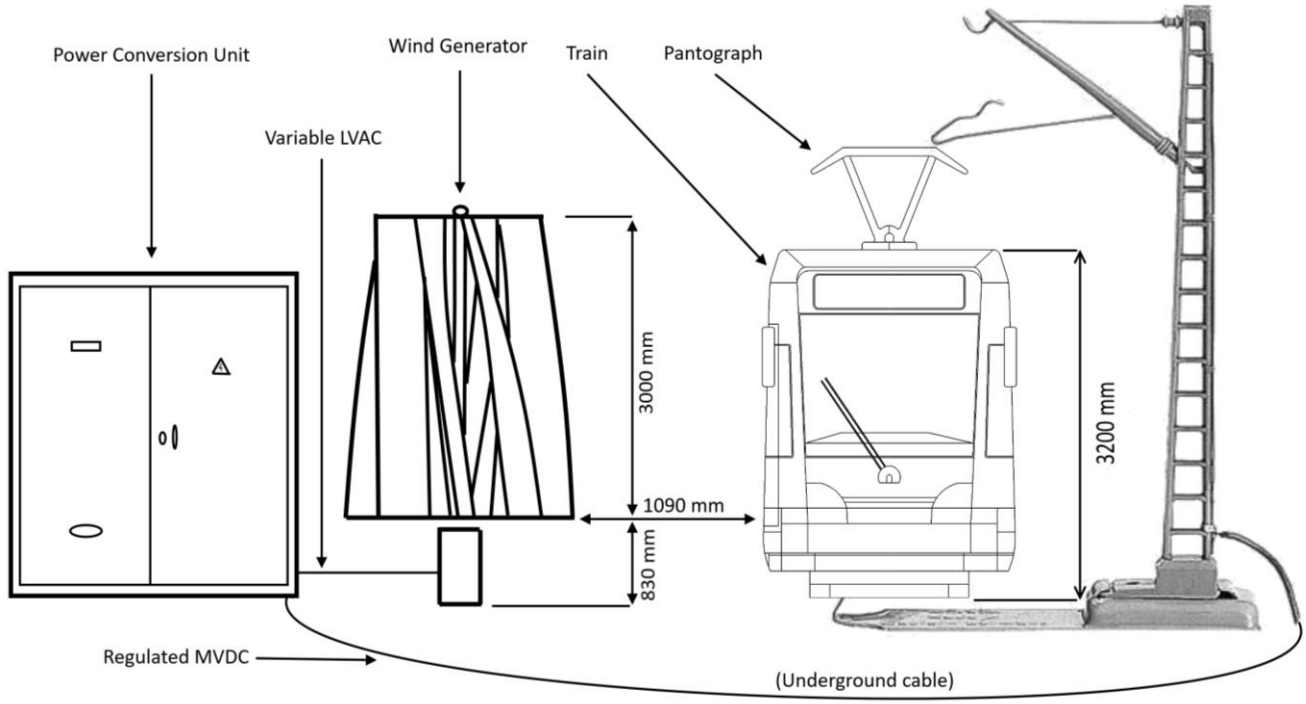

Fig. 2. Scheme of the VAWT installation with the power conversion unit and the train.

Once chosen the optimal location, wind resource has been studied.

B. Wind resource

In order to calculate the wind power output for each corresponding wind speed, the wind speed at the height of VAWTs is calculated by equation (1), given as:

$$v_{VAWT} = v_{ref} \frac{\ln\left(h_{VAWT} / z_0\right)}{\ln\left(h_{ref} / z_0\right)} \tag{1}$$

where v_{VAWT} is the wind speed at the height of the VAWTs [m/s], v_{ref} is the wind speed at the reference height [m/s], h_{VAWT} is the height of the VAWT [m], h_{ref} is the reference height [m] and z_0 is the surface roughness length [m].

The energy produced by the set of VAWTs is calculated by summing the multiplications of the power curve of each VAWT by the wind speed distribution.

The wind speed distribution is characterized by a two-parameter Weibull distribution. Equation (2) represents the Weibull probability density function, given as:

$$f(v) = \frac{k}{c}\left(\frac{v}{c}\right)^{k-1} \cdot \exp\left[-\left(\frac{v}{c}\right)^{k}\right] \tag{2}$$

where v is the wind speed [m/s], k is the Weibull shape factor and c is the Weibull scale parameter, which are obtained by the method of least squares [9].

III. Modelling of the Air Mass Displacement

The effect of the air mass displacement has been modelled by Finite Element Method (FEM). Initially, the geometry of the train has been implemented using a CAD (Computer Aided Design) program. In this case, the Solid Edge program has been used. Once the geometry has been defined, it is exported to COMSOL Metaphysics in IGES format. The domain of the train and the surrounding fluid, as well as the materials of which each element is composed have been defined. In the case of the train, the steel is used and in the case of the surrounding fluid, the air.

Fig. 3 shows the mesh of the train and the surrounding air in COMSOL environment, which consists of 1,826,825 domain elements, 66,222 outline elements, and 2,517 edge elements.

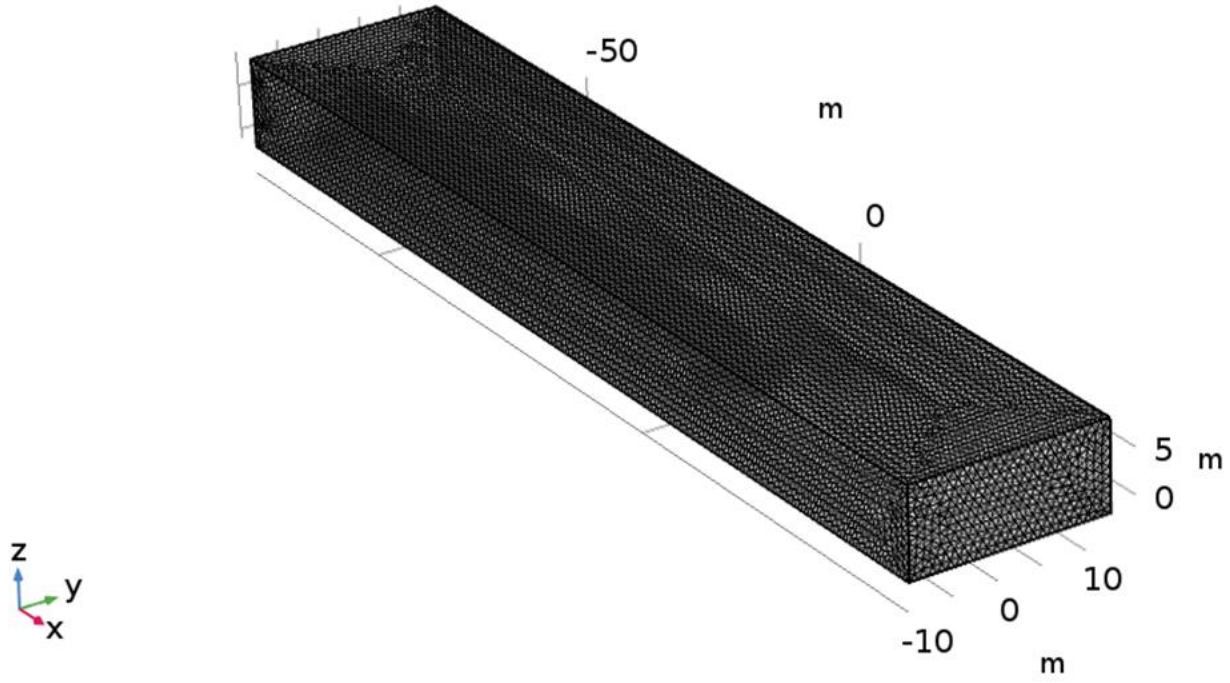

Fig. 3. Train and surroinding air gap structure (a) and mesh (b) in COMSOL environment.

To emulate the effect of air mass displacement a turbulent flow $k-\varepsilon$ model has been used, assuming incompressible flow. This formulation is suitable for single-phase flows at high Reynolds number [10]. The equations used to implement this model are based in the Reynolds-averaged Navier-Stokes (RANS) equation (3) for conservation of momentum and the continuity equation (4) for conservations mass. The flow near wall is modelled using wall functions.

$$\partial(u\cdot\nabla)u = \nabla\cdot\left[-pI + (\mu+\mu_T)\left(\nabla u + (\nabla u)^T\right)\right] + F \tag{3}$$

$$\partial\nabla\cdot(u) = 0 \tag{4}$$

where ∂ is the density [kg/m^3], u is the fluid velocity vector [m/s], ∇ is the fluid divergence, p is the fluid pressure [Pa], I is the matrix identity, μ is the dynamic viscosity of the fluid [Pa·s], F is the volume forces vector [N/m^3] and μ_T is the turbulent dynamic viscosity [Pa·s], given in equation (5).

$$\mu_T = \partial C_\mu \frac{\varepsilon^2}{k} \tag{5}$$

where C_μ is an experimental constant of the model, ε is the turbulent kinetic energy dissipation [m^2/s^3] and k is the turbulent kinetic energy [m^2/s^2]. Turbulence effects are modelled using the standard (6)-(7) equation of $k-\varepsilon$ model with realizability constraints [5].

$$\partial(u\cdot\nabla)k = \nabla\cdot\left[\left(\mu+\frac{\mu_T}{\sigma_k}\right)\nabla k\right] + p_k - \partial\varepsilon \tag{6}$$

$$\partial(u\cdot\nabla)k = \nabla\cdot\left[\left(\mu+\frac{\mu_T}{\sigma_\varepsilon}\right)\nabla \varepsilon\right] + c_{\varepsilon 1}\frac{\varepsilon}{k}p_k - c_{\varepsilon 2}\partial\frac{\varepsilon^2}{k} \tag{7}$$

where σ_k and σ_ε are the Prandtl Numbers for k and ε, respectively, $c_{\varepsilon 1}$ and $c_{\varepsilon 2}$ are experimental constants of the model and p_k is the production of turbulent kinetic energy due to efforts, given in equation (8).

$$p_k = \mu_T\left[\nabla u : \left(\nabla u + (\nabla u)^T\right)\right] \tag{8}$$

where the term ： represent a contraction, and in this case can be written as shown in equation (9).

$$\nabla u : \left(\nabla u + (\nabla u)^T\right) = \sum_n\sum_m \nabla u_{nm}\left(\nabla u + (\nabla u)^T\right)_{nm} \tag{9}$$

IV. Proposed Power Conversion System

This section describes the proposed power conversion system, which consists of an AC/DC and DC/DC converter per VAWT, and a SST common to all VAWTs. Fig. 4 shows the main scheme of the proposed topology to integrate the VAWTs into the train MVDC catenary.

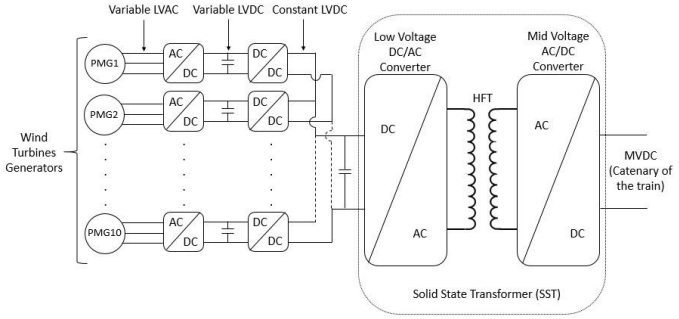

Fig. 4. Proposed power conversion system for the VAWTs integration.

The conversion from LVAC to MVDC has several stages. First of all, the power generated from the Permanente Magnet Synchronous Generator (PMSG) of the VAWTs is variable both in voltage and frequency, due to variations in wind speed. This voltage is named as variable LVAC in Fig 1. In order to overcome these variations, a three phase full-wave diode bridge rectifier converts the generated power in variable LVDC. In equation (10) the output mean voltage $V_o(avg)$ of the rectifier in function of the input single-phase voltage V_{phs}.

$$V_o(avg) = 2\cdot\hat{V}_{phs}\cdot\frac{\sin\left(\pi/3\right)}{\pi/3} = \frac{3\cdot\sqrt{3}}{\pi}\hat{V}_{phs} \tag{10}$$

Despite obtaining the generated power in LVDC, this is not suitable for connecting all the VAWT in parallel, since it is variable. Therefore, the next step is to convert the variable LVDC to constant LVDC by a boost converter. This control is achieved by calculating the duty cycle D according to fixed output voltage V_{out} and variable input voltage V_{in}, as given in equation (11).

$$D = 1 - \frac{V_{in}}{V_{out}} \tag{11}$$

This constant LVDC is the link where other sources are connected. The boost control has been carried out with a voltage feedback loop and a PI controller.

Fig. 5 shows this first stage of power conditioning, which is applied to the output of each generator of the 10 VAWTs.

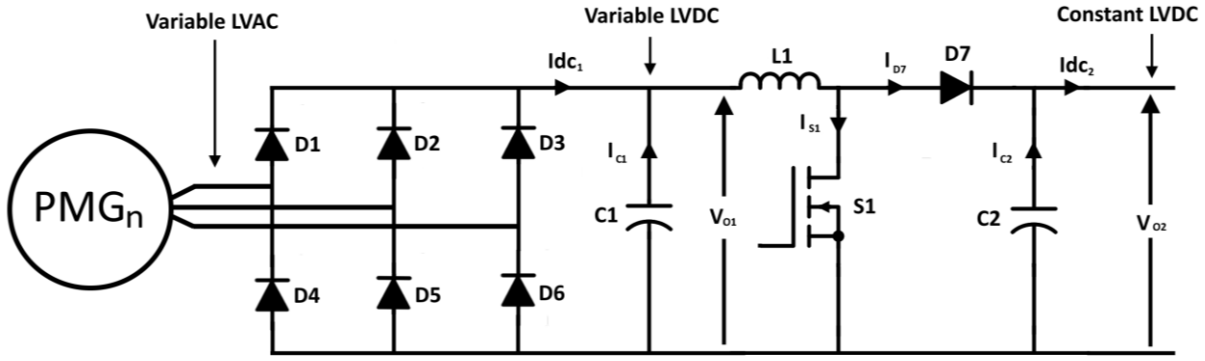

Fig. 5. LVAC-LVDC stage used to couple each PMG with the SST.

Once the sources inject their generated power to the fixed LVDC link, a solid state transformer (SST) converts it to a MVDC, as shown in Fig. 6. The SST consists of a single-phase full bridge inverter, a high frequency transformer (HFT) and a single-phase full-wave rectifier. The inverter generates a high-frequency square waveform (SQW) that is amplified and transferred to the output rectifier by means of the HFT. In this way, in addition to exchanging high voltage ratios, the HFT also provides galvanic isolation of the generation system. A carrier frequency of 10 kHz has been used to control the full bridge inverter.

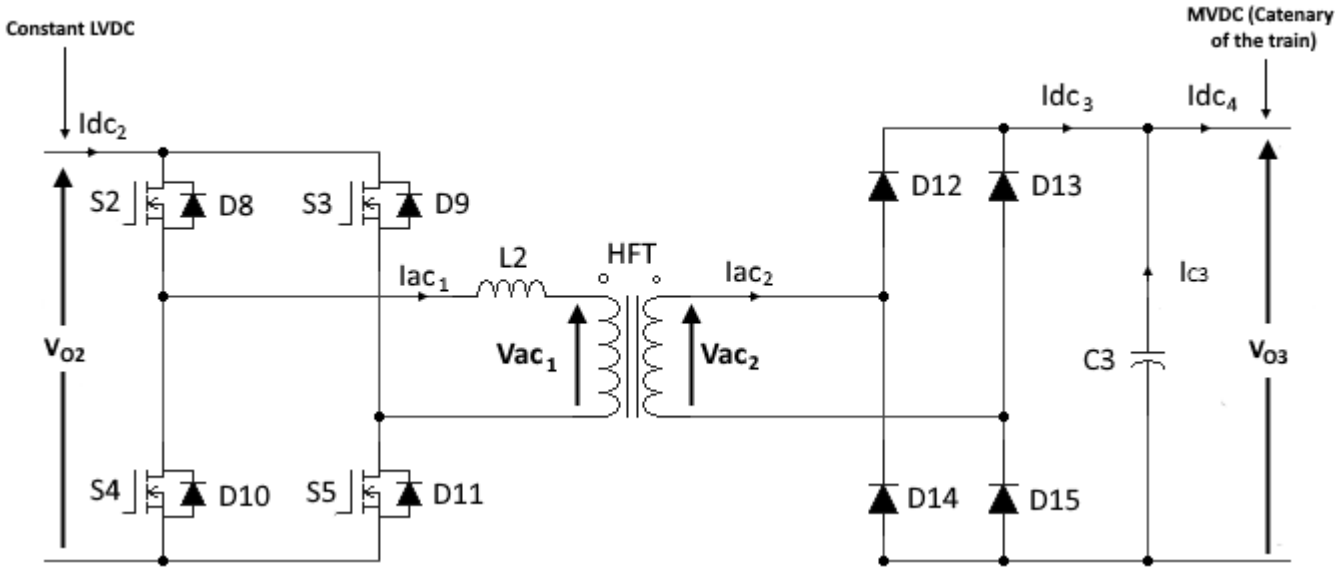

Fig. 6. Isolation stage based on SST with a SQW inverter and a single-phase full wave bridge rectifier.

Equation (12) and (13) show the calculation of the output voltage in function of the input voltage, for the case of the single-phase full bridge inverter and the single-phase full wave rectifier, respectively.

$$\hat{V}_o = \frac{4}{\pi} V_{in} \tag{12}$$

$$V_o(\text{avg}) = \frac{\sin(\pi/2)}{\pi/2} V_{in} \tag{13}$$

V. Main Results

This section describes the main results obtained regarding the wind potential, the electrical energy production and the system integration to the MVDC catenary through the proposed power conversion system.

A. *Potential of the air mass displaced*

Fig. 7 shows the results of a stationary CFD simulation with a train velocity of 80 km/h and an average wind speed and a predominant direction of 5.02 m/s and 285 degrees (North reference), respectively.

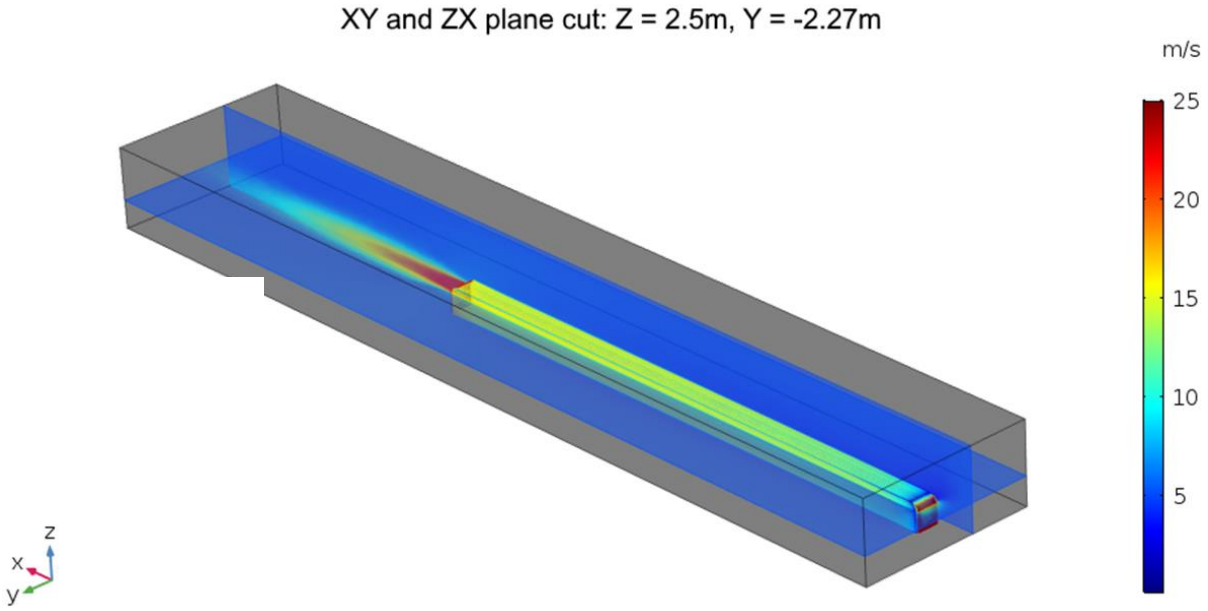

Fig. 7. XY and ZX plane cut (a) in the optimal location of the VAWTs.

As can be seen in Fig. 7, the displacement of the train generates a mass of air that extends slightly towards the sides, being the greater wind speed in the rear part of the train, which will produce the drag force. The ideal would be to locate the VAWT as close to the train as possible, always maintaining the established safety distance, which in this case is 1090 mm. In this sense, a cut of the ZX plane has been made at 1,090 mm plus the radius of the VAWT (1,180 mm) and a cut of the XY plane, at the height that will be located the center of the VAWT (2,500 mm). The wind speed obtained in the cut of the two ZX and ZY planes is 7,739 m/s.

B. *Electrical energy production*

Two aspects have been taken into account for the generation of electric power. On the one hand, the electric power produced by the VAWTs taking advantage of the wind potential of the place. On the other hand, the available energy due to the mass of air displaced by the moving train.

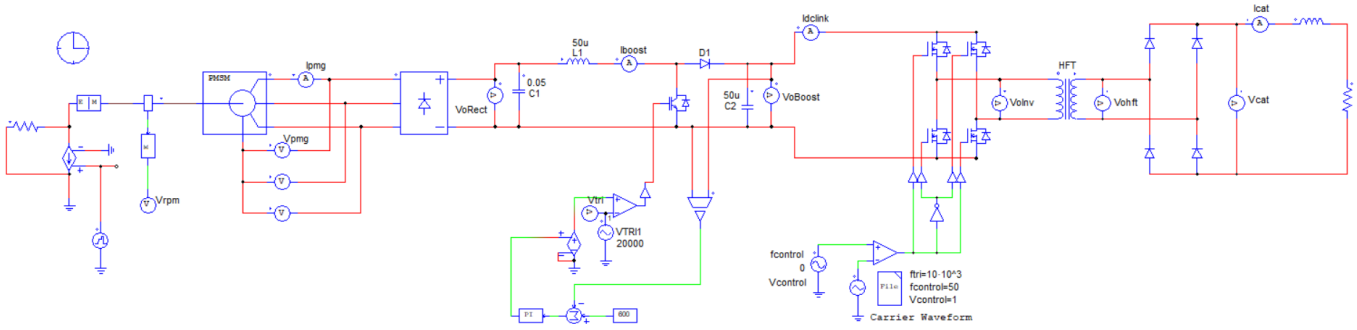

Fig. 8. Scheme of the topology simulated in PSIM environment.

For the first case, the expression (1) has been evaluated for the entire data history of available wind speed, obtaining as a result a wind speed velocity vector at the desired height, which in this case is 2.5 m. This vector has been evaluated by expression (2), obtaining as a result the Weibull distribution. Finally, to calculate the electrical power generated, the Weibull distribution and the power curve of each VAWT shown in Fig. 10 have been multiplied. As a result, taking into account the production of all VAWTs, a total energy of 67.53 MWh/year has been obtained.

Fig. 9 shows the power curve of the chosen VAWT, developed by Kliux energies [5]. It can be seen how the power produced by the VAWT increases from 497 W to 1,297 W when the effect of the displacement of the air mass occurs.

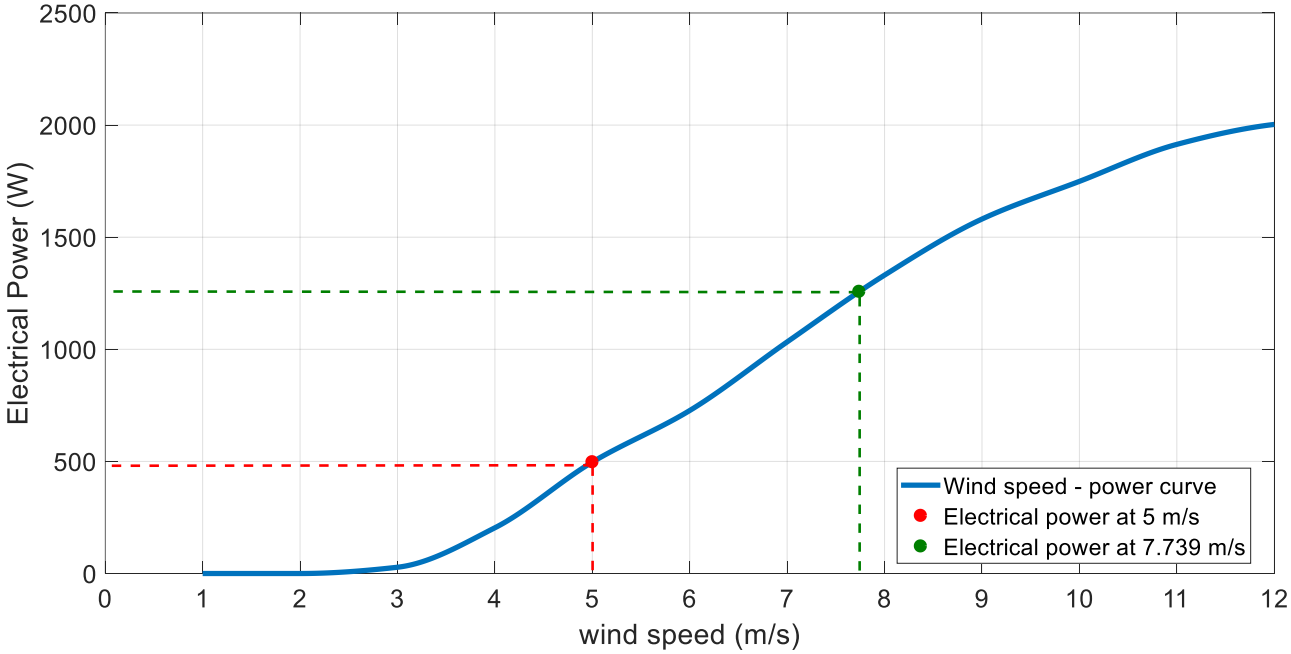

Fig. 9. Wind speed-power curve, and mean power generated with and without air mass displacement by the train.

To calculate the power generated harnessing the air mass displaced, it is necessary to take into account the time during which the wind speed of the mass of air displaced by the train is maintained. Since in this case only stationary simulations have been carried out, estimated data from the MACE project have been used [6]. In that project, researchers found that the wind trail remained for a time of 147 s once the train passed. On the other hand, the frequency with which the train passes at the chosen location has been taken into account. In this sense, the train passes a total of 41,040 times a year through that location. The results obtained show an energy recovery of 12.3 MWh/year, assuming all trips made by the train and that the VAWTs were operating with an average wind speed of 5.02 m/s before the train passed. Table I shows the total electric power produced for both cases, under normal conditions and when the displacement of the air mass occurs.

TABLE I. ESTIMATION OF ELECTRICAL ENERGY PRODUCTION.

Conditions	***Energy production per VAWT***	***Total energy production***
Energy production without train displacement	18.5 kWh/day	67.53 MWh/year
Energy production by mass displacement	3.37 kWh/day	12.3 MWh/year
Total energy production	21.87 kWh/day	79.83 MWh/year

The total energy obtained represents 0.11% of the total annual consumption of all the facilities of the subway (72.575 GWh/year).

C. System integration to catenary

Fig. 8 shows the LVAC-MVDC proposed topology in PSIM environment.

Fig. 10 shows the results of the simulation of the power production of one VAWT when the train is displacing the air mass. As can be seen, the rotational speed of the generator increases when the train displaces the mass of air, which causes the increase of the voltage and current generated in amplitude and frequency.

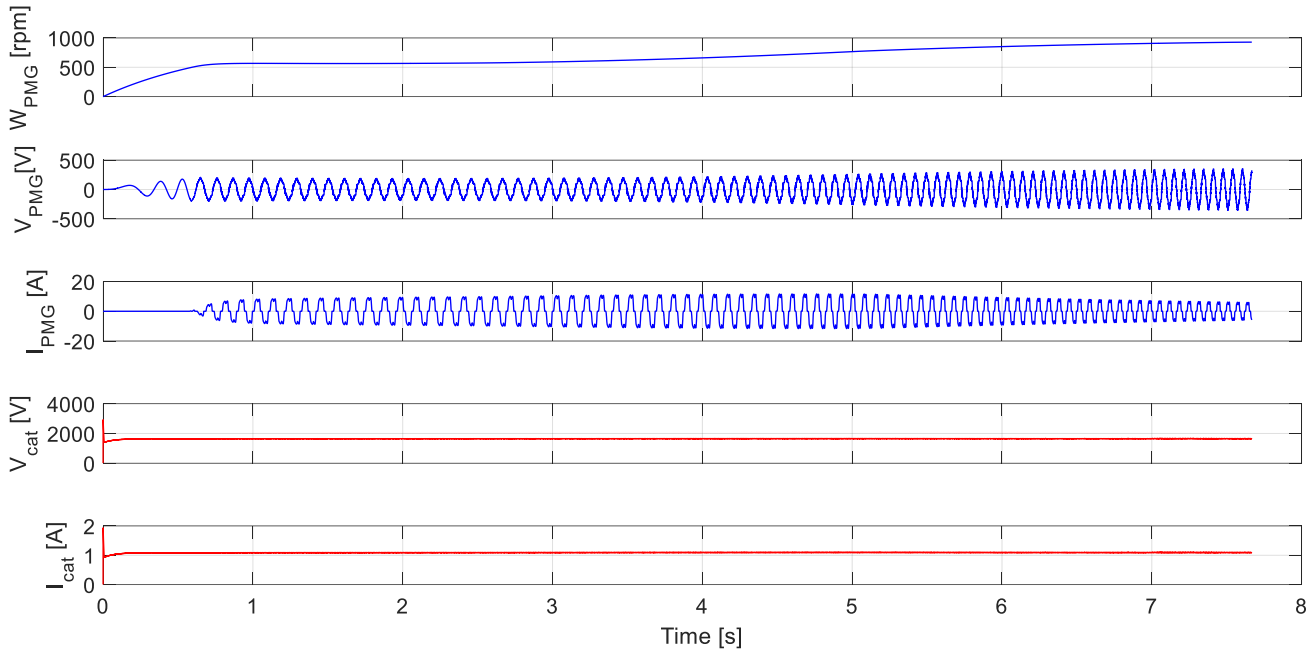

Fig. 10. PMG speed, voltage and current and voltage and current in the catenary.

Fig. 11 shows the PMG speed and voltage current at the output of the rectifier. Fig. 12 shows the current through the diode of the boost converter and the voltage and current at the DC link. The voltage and current of the DC bus manages to remain constant despite the variations caused by the gust of wind.

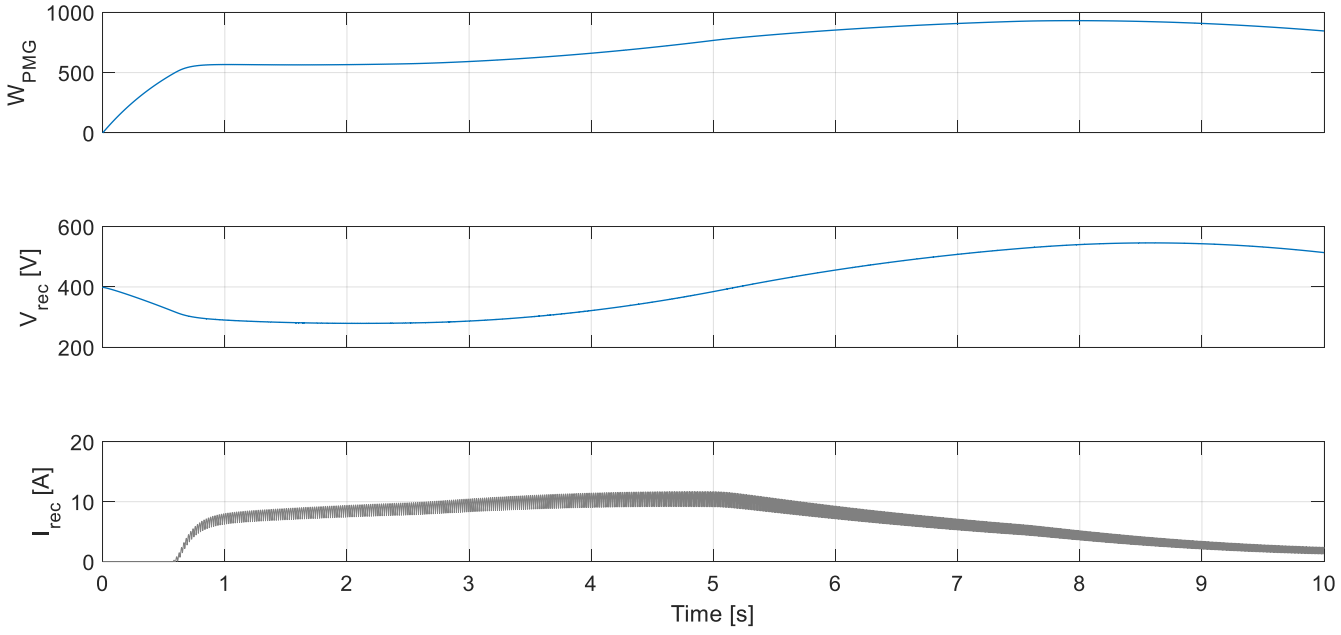

Fig. 11. PMG speed and voltage and current at the output of the rectifier.

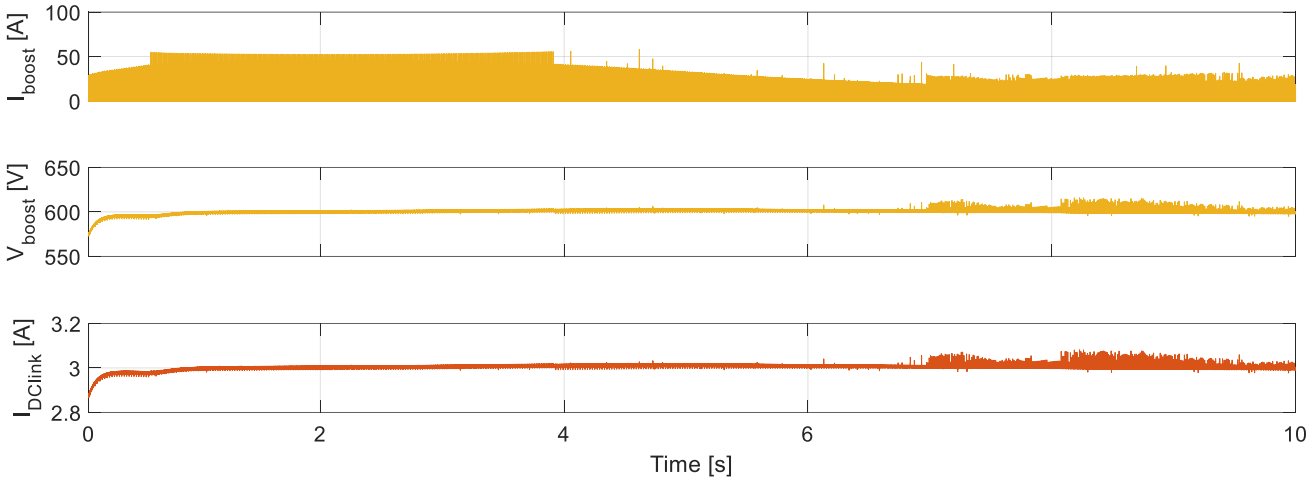

Fig. 12. Current and voltage at the boost and current at the DC link.

VI. Conclusions

This paper has proposed a system for harnessing the available wind potential due to the mass of air displaced by a moving train. The methodology carried out to replicate this study in another location has been shown. Likewise, it has been proven that the set of 10 VAWTs with a nominal power of 1.8 kW each has been able to produce a total of 79.83 MWh / year, of which 12.3 MWh / year correspond to the effect of the displacement of the air mass.

The topology for the proposed integration allows to easily integrate any DER in a MVDC system. In addition, by using a dual active bridge in the SST configuration, it could be even recovered energy by regenerative braking or integrate storage systems together with the catenary system.

As a future development of this proposal, it is proposed to replace the simple rectifier of each generator with a controlled rectifier and develop an individual MPPT control for each turbine in order to extract the maximum power at all times. In addition, it is proposed to compare the topology proposed for the integration of the generation system into the catenary with other existing ones in order to analyze the advantages and disadvantages that presents.

It can be concluded that the proposed system makes optimal use of the total available energy. In this way, the proposed system allows the train to recover in the form of electrical energy part of the mechanical energy lost due to friction with the air during its displacement.

Acknowledgment

The authors thank the support from the Spanish Ministry of Economy, Industry and Competitiveness (project ENE2016-79145-R AEI/FEDER, UE), the Basque Government (project ELKARTEK KK-2017/00083 and GISEL research group IT1083-16), as well as from the University of the Basque Country UPV/EHU (project EHUA15/25 and research group funding PPG17/23).

References

[1] Siavash Ebrahimi, Michael Mac Kinnon, Jack Brouwer, California end-use electrification impacts on carbon neutrality and clean air, Applied Energy, vol 213, pp 435-449, 2018.

[2] W. Liu, J. Xu and J. Tang, "Study on control strategy of urban rail train with on-board regenerative braking energy storage system," *IECON 2017 - 43rd Annual Conference of the IEEE Industrial Electronics Society*, pp. 3924-3929, Beijing, 2017.

[3] G. M. Scheepmaker and R. M. P. Goverde, "Energy-efficient train control including regenerative braking with catenary efficiency," *2016 IEEE International Conference on Intelligent Rail Transportation (ICIRT)*, pp. 116-122, Birmingham, 2016.

[4] L. Pugi, A. Frilli, D. Nocciolini, E. Meli and A. Rindi, "Development and validation of a model for the optimization of regenerative braking of high speed trains," *2016 IEEE 16th International Conference on Environment and Electrical Engineering (EEEIC)*, pp. 1-6, Florence, 2016.

[5] C. Baker, "*The flow around high speed trains*," J. of Wind Engineering and Industrial Aerodynamics, Vol. 98, pp. 277-298, 2010.

[6] WWT Tunnel Official Website. MACE Project. Link: http://www.wwttunnel.com/lacmta.html Last accesed on 21/05/2018.

[7] Q. Song, B. Zhao, J. Li and W. Liu, "An Improved DC Solid State Transformer Based on Switched Capacitor and Multiple-Phase-Shift Shoot-Through Modulation for Integration of LVDC Energy Storage System and MVDC Distribution Grid," in *IEEE Transactions on Industrial Electronics*, vol. 65, no. 8, pp. 6719-6729, Aug. 2018.

[8] Global wind atlas 3.0 provided by IRENA. Available: https://irena.masdar.ac.ae/gallery/#map/103

[9] M. Celeska, K. Najdenkoski, V. Stoilkov, A. Buchkovska, Z. Kokolanski and V. Dimchev, "Estimation of Weibull parameters from wind measurement data by comparison of statistical methods," IEEE EUROCON 2015 - International Conference on Computer as a Tool (EUROCON), Salamanca, pp. 1-6, 2015.

[10] J.F. Douglas, J.M. Gasiorek, J.A. Swaffield, "*Fluid Mechanics*," Prentice Hall, 2001.

[11] Kliux Geo 1800 catalog. Kliux energies. Available:
http://www.kliux.com/wp-content/uploads/2011/04/KLIUX_cat_en.pdf

[12] D. Kuzmin, O. Mierka, and S. Turek, "On the implementation of the *k*-ε Turbulence Model in Incompressible Flow Solvers Based on Finite Element Discretization," Int.J. Computing Science and Mathematics, vol. 1, pp. 193–206, 2007.